An alternative carbon source from cassava residue saccharification liquid for in-situ fabrication of polysaccharide macromolecule/bacterial cellulose composite hydrogel: A comparative study

Li Ji, Wenwen Xue, Liwei Zhu, Jianxin Jiang*

Department of Chemistry and Chemical Engineering, MOE Engineering Research Center of Forestry Biomass Materials and Bioenergy, National Forest and Grass Administration Woody Spices (East China) Engineering Technology Research Center, Beijing Forestry University, Beijing 100083, China

* *Corresponding author. E-mail address: jiangjx2004@hotmail.com; Tel.: +86-10-6233-8267.*

1. Materials
2. Preparation of CSL
3. In vitro cell cytotoxicity assay
4. SA and SH contents during the in-situ process
5. Structural parameters calculated from XRD data
6. Hydrogel morphology
7. Structural characterization
8. Tensile and swelling properties
9. In vitro drug-release studies
10. In vitro cytotoxicity
11. Reference

1. Materials

Cassava residue (CR) was kindly provided by Guangxi Minyang Starch Factory (Guangxi Province, China), which contained 52.6% of starch, 29.0% of cellulose and 6.1% of acid-soluble lignin. AX (ATCC23767) was purchased from Guangdong Microbial Culture Collection Center (GDMCC, Guangdong Province, China). The α-amylase and glucoamylase used in the saccharification process were commercial enzymes from Beijing Aoboxin Co., Ltd (Beijing, China), and the enzyme activities were 4 KU/g and 100 KU/g, respectively. Bovine serum albumin (BSA), yeast extract, peptone, dibasic sodium phosphate and citric acid monohydrate were bought from Aladdin Biochemical Technology Co., Ltd (Shanghai, China). Sodium alginate (SA, specification: purity of 90%, mannuronate/guluronate ratio of 1, molecular weight of 430 kDa) was purchased from Macklin Biochemical Technology Co., Ltd (Shanghai, China). Sodium hyaluronate (SH, specification: purity of 92%, glucuronic acid ≥ 43%, molecular weight of 1500 kDa) was bought from Shandong Freda Biotechnology Co.,Ltd (Shangdong Province, China). Cellic Ctec2 was gifted by Novozymes Investment Co., Ltd. (Beijing, China), and was a complex mixture. The filter paper activity of Cellic Ctec2 was 160 FPU/mL, and the contained cellobiase activity was 24 CBU/mL.

2. Preparation of CSL

The saccharification liquid of CR-starch was performed in a 500-mL conical flask with 20 % dry matter (Ji et al., 2016). The commercial α-amylase was at a loading of 150 u/g-CR and glucoamylase dosage was of 20 u/g-CR. The saccharification liquid of CR-cellulose was carried out in the enzymatic hydrolysis system of 100 mL with substrate concentration of 2% (w/v) using commercial enzyme cellulase (Cellic Ctec2, Sigma Co., St. Louis, MO, USA). The dosage of Cellic Ctec2 was 18 FPU/g cellulose. The hydrolysis experiments were performed in the acidic buffer solution of pH 4.8 at 48 °C and 150 rpm for 72 h. The saccharification liquids of CR-cellulose and CR-starch were mixed with the main composition of 93.6% glucose and a small amount of soluble lignin. The concentrated saccharification liquid was added to the medium as carbon source for the preparation of SA-BC/SH-BC composite hydrogels with the glucose concentration of 400 g/L.

3. In vitro cell cytotoxicity assay

As the first human cell line, Hela cells have the high amplification activity with the superior proliferative capacity. Hela cells are able to propagate indefinitely and they are one of the most widely used cell lines for biocompatibility test (Yuan et al., 2018; Kim et al., 2019). Hela cells (RCB0007) were provided by Daxing Biological Pharmaceutical Industry Base (Beijing, China). They were used to examine induced cytotoxicity in the composite BC hydrogels using the MTT assay (Cui et al., 2015). The cells were cultured in DMEM medium including 1% penicillin-streptomycin and was kept in an incubator at 37 °C with 5.0% CO_2 atmosphere. The cells were transferred every 3–4 days with the replenished medium every 2–3 days.

4. *SA and SH contents during the in-situ process*

Table S1. The contents of SA and SH during the in-situ microbial synthesis system.

Samples	Concentration of SA (wt%)	Concentration of SH (wt%)
BC	0	0
SA-BC-0.25	0.25	
SA-BC-0.5	0.5	-
SA-BC-1.0	1.0	
SH-BC-0.25		0.25
SH-BC-0.5	-	0.5
SH-BC-1.0		1.0

5. *Structural parameters calculated from XRD data*

Table S2. Structural parameters calculated from XRD data.

Samples	Index of crystallinity (CrI)/%	Full width at half maxium (FWHM)/rad	Crystallite size/nm
BC	58.18	1.49	5.42
SA-BC-0.25	49.36	1.51	5.34
SA-BC-0.5	45.92	1.54	5.28
SA-BC-1.0	42.63	1.63	5.19
SH-BC-0.25	53.77	1.50	5.36
SH-BC-0.5	47.63	1.52	5.33
SH-BC-1.0	46.58	1.53	5.29

6. Hydrogel morphology

The morphologies of SH-BC-0.25, SH-BC-0.5, SA-BC-0.25 and SA-BC-1 were observed using SEM, see Figure S1. It is clear that the supplemented macromolecules of SA and SH constructed the 3D network without obvious aggregation. Compared to SH-BC-1 and SA-BC-0.5, the average nanofibres diameter of the presented samples decreased to 20–35 nm. However, the net-like structure of the hydrogel samples disappeared and distributed the line-shaped structure with the increasing SA content to 1%.

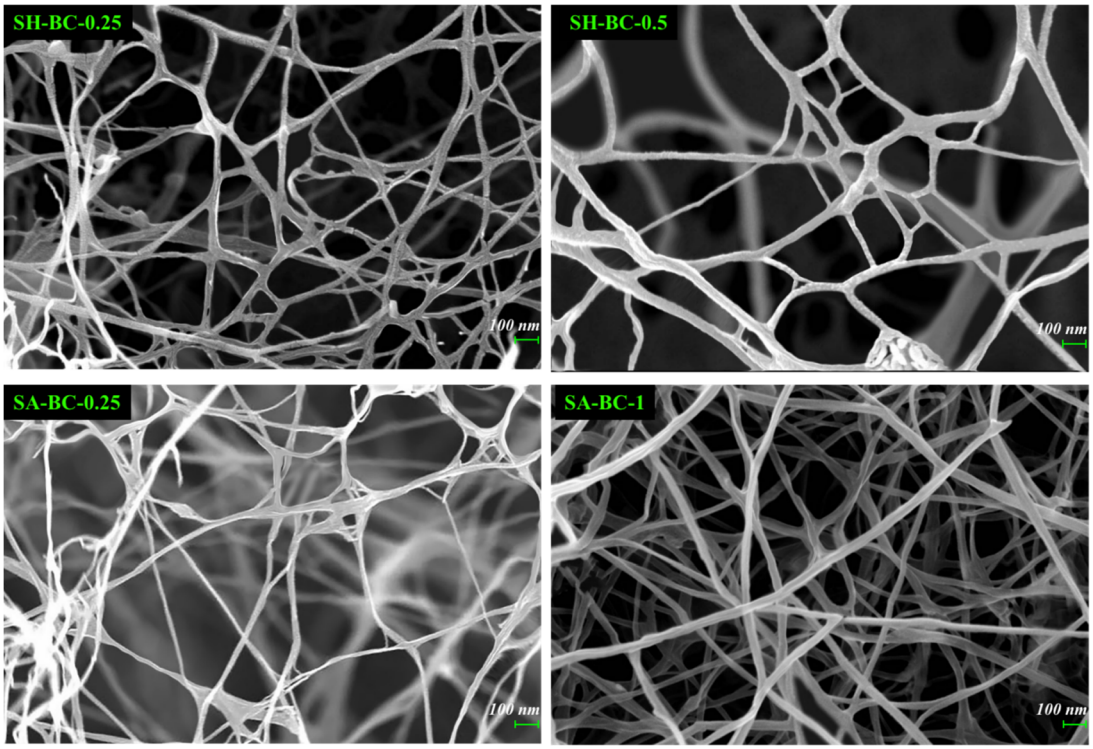


Figure S1 SEM images of SH-BC-0.25, SH-BC-0.5, SA-BC-0.25, and SA-BC-1.

7. Structural characterization

The FT-IR spectra of SH-BC-0.25, SH-BC-0.5, SA-BC-0.25 and SA-BC-1 is shown in Figure S2A. In the composite SH-BC hydrogel spectrum, the stretching of C-O at 1161 cm^{-1} was different compared with that of the native BC. And the bending of N-H at 870 cm^{-1} confirmed the crosslinking behaviors of SH and BC (Franca et al., 2009). In the composite SA-BC hydrogel spectrum, the stretching of C-O at 1641 cm^{-1} presented differently reveals the linkage of SA and BC was formed compared with the native BC. Furthermore, the broad peaks, as known as the red-shift of hydrogen bond at 3000–4000 cm^{-1} were assigned to the intermolecular hydrogen bonds between BC and SA/SH (Yan et al., 2018). Figure S2B exhibits the XRD spectra of the four hydrogel samples, the observed $(1\bar{1}0)$, (110) and (200) planes at 14.6° and 16.9° and 22.7° demonstrated that SA or SH mostly incorporated with BC in the amorphous domains (Gaspar et al., 2014; Gao et al., 2019). In addition, the quantified crystal data shown in Table S2 demonstrated that the interfered SA and SH would reduce the CrI of BC chains (Kim, et al. 2017). The increasing dosage of SA resulted in the lower initial decomposition temperature of SA-BC hydrogels and SA-BC-1 presented the poorest thermal stability with the lower decomposition temperature (Figure S2C). Also, as shown from DTG curves (Figure S2D), SH-BC hydrogels displayed a better thermal stable property compared to SA-BC hydrogels, possibly because of the higher amorphous cellulose content and the decreased crystallinity of SA-BC.

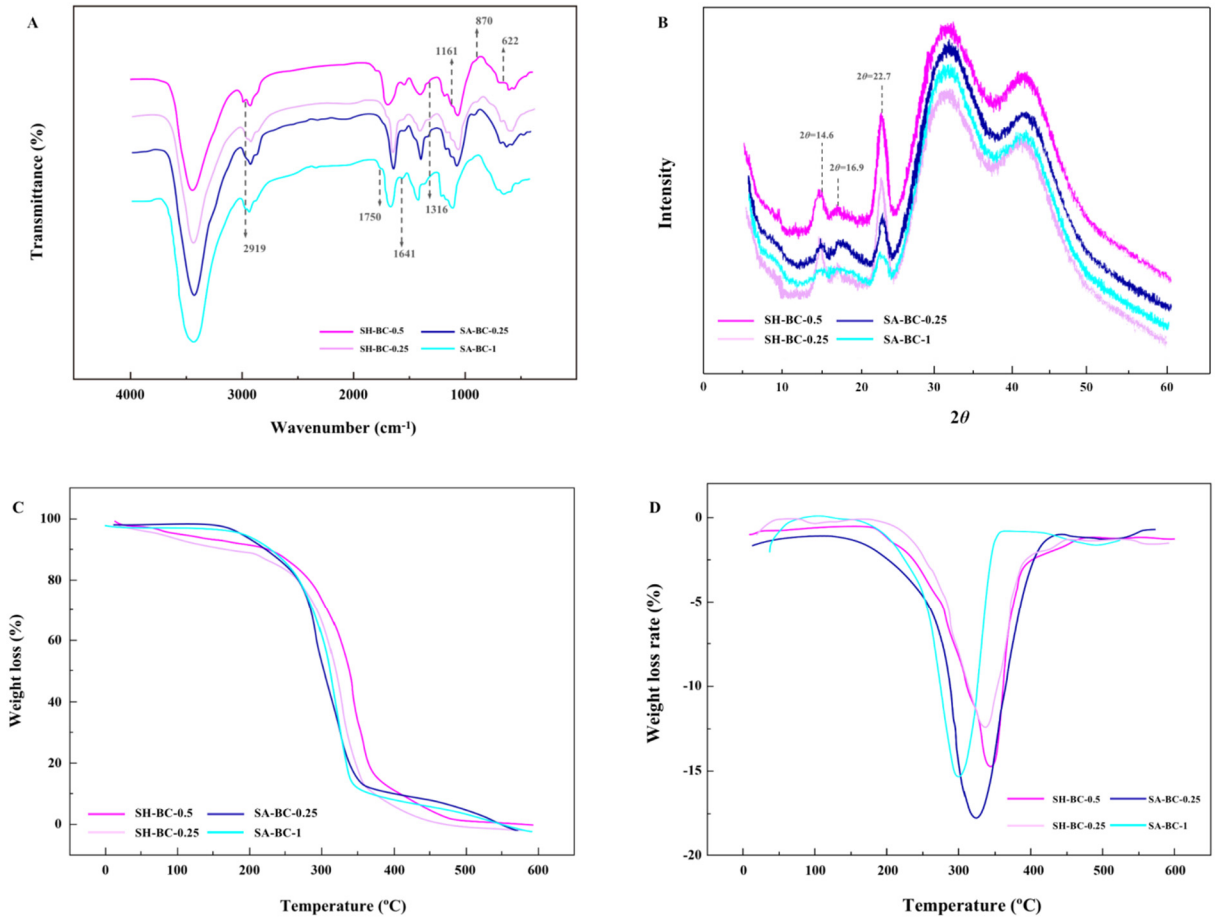


Figure S2 Structural characterization of SH-BC-0.25, SH-BC-0.5, SA-BC-0.25, and SA-BC-1: FT-IR (A); XRD (B); TGA (C) and DTG (D).

8. Tensile and swelling properties

The testing results of tensile strength of SH-BC-0.25, SH-BC-0.5, SA-BC-0.25 and SA-BC-1 are shown in Figure S3A, respectively is 0.79, 1.07, 0.63 and 0.51 MPa at strains of 452%, 529%, 433% and 378%, respectively. The improved tensile strength was attributed to the incorporation of SA or SH in the culture medium with BC through hydrogen bonding. These tensile strengths were quantitatively evaluated using the striking enhancement, but the excessive amount of 1% SA might lead to the brittleness of the composite hydrogel. This low tensile strength of SA-BC-1 would lead to its relatively poor mechanical property. The experimental results further validated that SH-BC had better mechanical property compared to SA-BC and the mechanical property of SH-BC was improved with the increasing dose of SH from 0.25% to 1%.

The swelling capacity of SH-BC-0.25, SH-BC-0.5, SA-BC-0.25 and SA-BC-1 hydrogels were determined (Figure S3B). The swelling rate of hydrogel samples increased obviously during the first 16 h. The hydrogel samples of SH-BC-0.25, SH-BC-0.5 and SA-BC-0.25 displayed better swelling performance than that of SA-BC-1 in the pH 7.4 buffer solution, and the equilibrium SRs were 7673%, 7976%, 8347%, and 2603% respectively. SH and SA contain numerous hydrophilic carboxyl groups forming hydrogen bonds with water, enhanced the thereby promoting water-sorption. The SR of SH-BC-0.25 was lower than those of SA-BC-0.25 because of the extra pore structure observed in SEM could increase inner specific surface area (Hu et al., 2014). However, when 1% of SA was added, the formed linear structure made it lose the advantage in the swelling behavior.

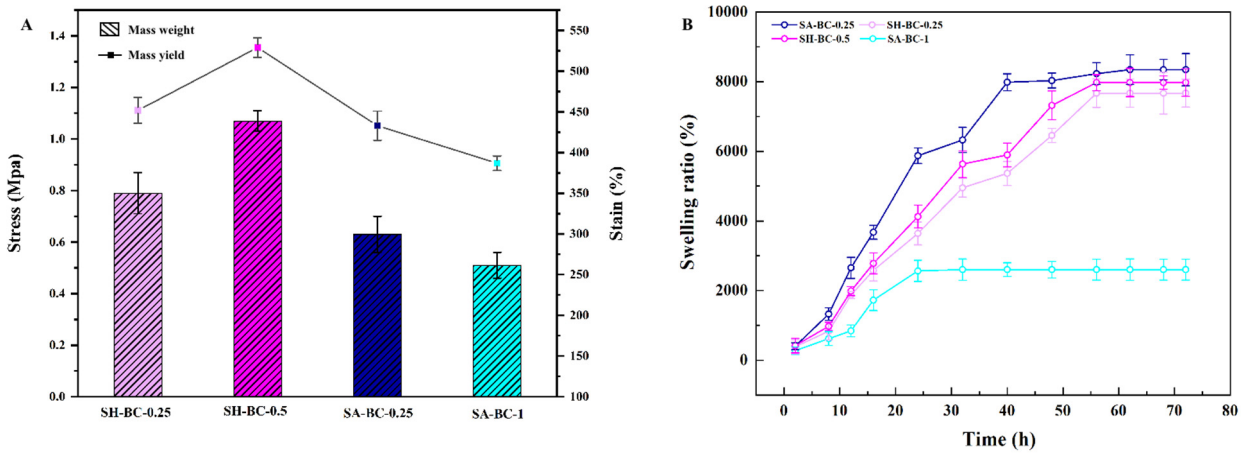


Figure S3 Tensile strength (A) and SR (B) of SH-BC-0.25, SH-BC-0.5, SA-BC-0.25, and SA-BC-1.

9. In vitro drug-release studies

The in vitro BSA accumulation releasing curves of the four hydrogel samples in SGF, SIF, and PBS at pH values of 1.2, 6.8, and 7.4 are shown in Figure S4. The entrapment efficiency (EE) of SH-BC-0.25, SH-BC-0.5, SA-BC-0.25 and SA-BC-1 for BSA were 33.68 ± 0.57%, 34.92 ± 0.83%, 36.04 ± 0.21% and 22.07 ± 0.46%, respectively. SA-BC-0.25 with smaller pores and more fibrous layers presented in the SEM images exhibited the better sustained-release effect, while SA-BC-1 lacked a porous network structure showed a limited drug release for BSA. Furthermore, the maximum cumulative release of the loaded BSA was reduced with the decrease in pH value from 7.4 to 1.2. For SH-BC-0.5, the percentage of 83.24% was shown at pH 7.4, 76.55% at pH 6.8 and 70.58% at pH 1.2, respectively. For SA-BC-0.25, the value showed as 84.12% at pH 7.4, 73.40% at pH 6.8 and 69.10% at pH 1.2, respectively. But no remarkable difference was found for SA-BC-1. Zeta potentials of SH-BC-0.25, SH-BC-0.5, SA-BC-0.25 and SA-BC-1 are exhibited in Figure S4E. Owing to the dissociated carboxyl group into $-COO^-$ at the alkaline pH value of 7.4, a declining trend was observed in zeta potential value of all the hydrogel samples (Ullah et al., 2016).

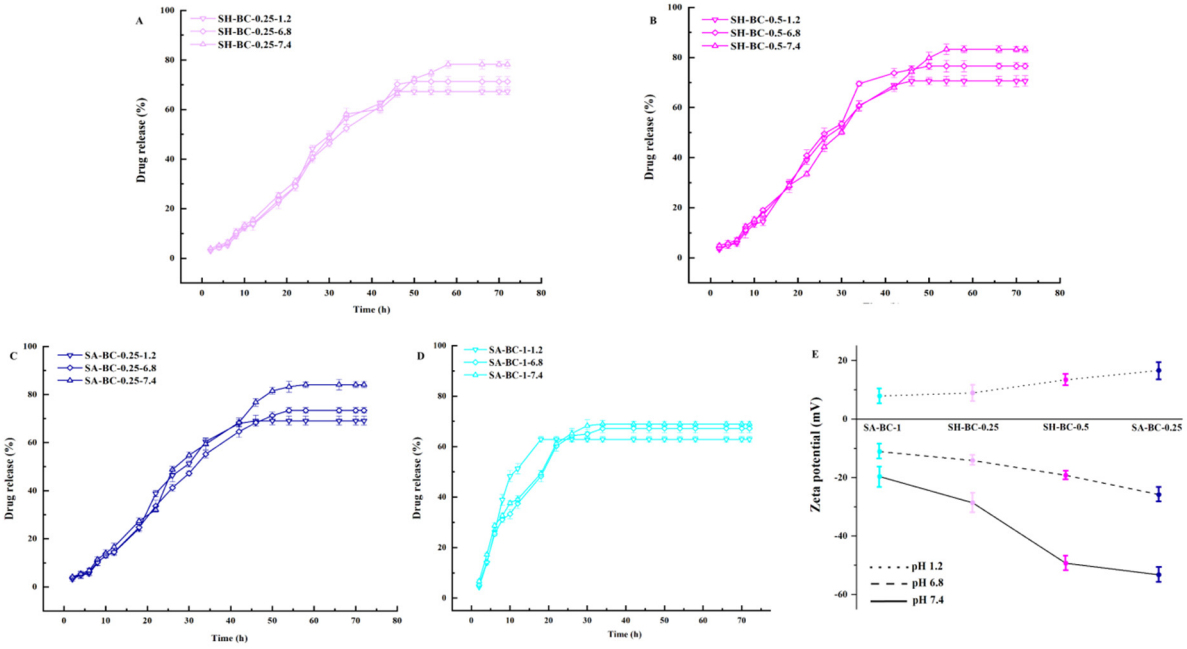


Figure S4 Profiles of the in vitro drug release efficiency (A) SH-BC-0.25, (B) SH-BC-0.5, (C) SA-BC-0.25, (D) SA-BC-1 and (E) zeta potential.

10. In-vitro cytotoxicity

The biocompatibility of biomaterials is crucial for clinical applications. Hela cells have been used as cell line model to evaluate the in vitro cytotoxicity of BC and the composite hydrogel products by direct and indirect methods (Xu et al., 2012). After 48 h growing in the medium containing the hydrogel products, the normal Hela cells with a nearly constant number were examined by optical microscopy (Figure S5). Besides, the morphology of the cells maintained unchanged after cell cultivation, indicating that the hydrogel product would not hamper the cells growth. MTT assay was used to determine the Hela cell viability in different concentrations of samples and the results were shown in Figure S5. After 48 h growing, cell viability was maintained the same to the control and no noted difference was found under different concentrations.

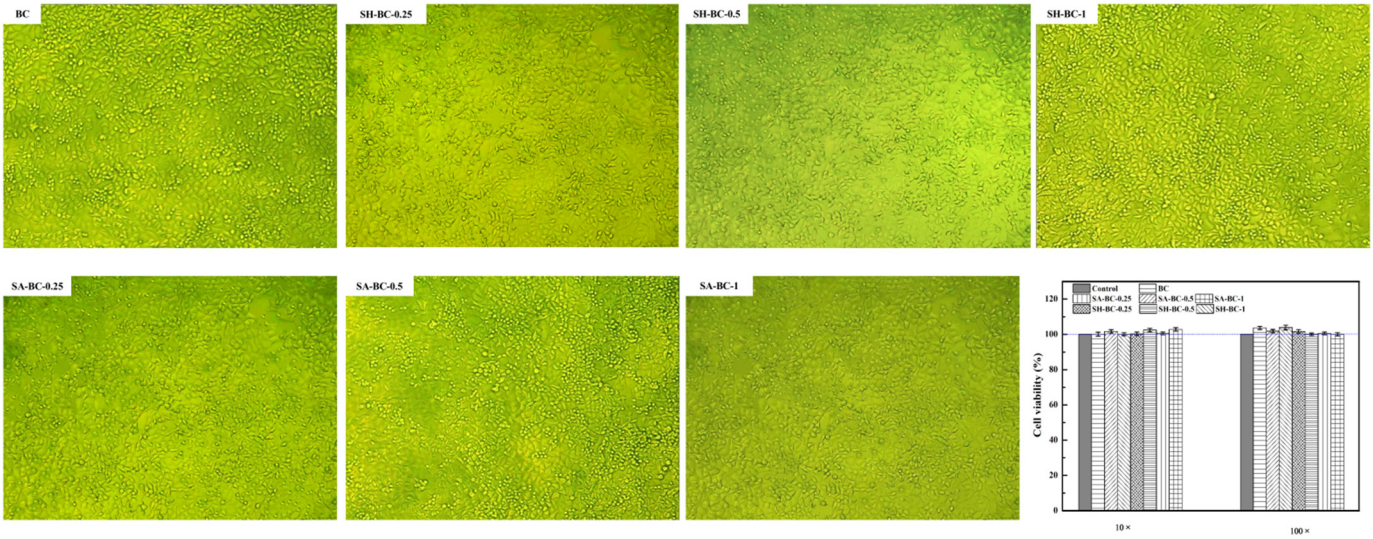


Figure S5 The cytotoxicity measure of BC, SH-BC-0.25, SH-BC-0.5, SH-BC-1, SA-BC-0.25, SA-BC-0.5 and SA-BC-1.

11. Reference

Cui, N., Qian, J., Liu, T., Zhao, N., & Wang, H. (2015). Hyaluronic acid hydrogel scaffolds with a triple degradation behavior for bone tissue engineering. Carbohyd. Polym. 126, 192-198.

Franca, C. A., Etcheverry, S. B., Pis Diez, R., & Williams, P. A. (2009). Irbesartan: FTIR and Raman spectra. Density functional study on vibrational and NMR spectra. Journal of Raman Spectroscopy: An International Journal for Original Work in all Aspects of Raman Spectroscopy, Including Higher Order Processes, and also Brillouin and Rayleigh Scattering, 40(9), 1296-1300.

Gao, M., Li, J., Bao, Z., Hu, M., Nian, R., Feng, D., ... & Zhang, H. (2019). A natural in situ fabrication method of functional bacterial cellulose using a microorganism. Nat. Commun. 10(1), 1-10.

Gaspar, D., Fernandes, S. N., De Oliveira, A. G., Fernandes, J. G., Grey, P., Pontes, R. V., ... & Fortunato, E. (2014). Nanocrystalline cellulose applied simultaneously as the gate dielectric and the substrate in flexible field effect transistors. Nanotechnology 25(9), 094008.

Hu, X., Feng, L., Xie, A., Wei, W., Wang, S., Zhang, J., & Dong, W. (2014). Synthesis and characterization of a novel hydrogel: salecan/polyacrylamide semi-IPN hydrogel with a desirable pore structure. J. Mater. Chem. B. 2(23), 3646-3658.

Ji, L., Zheng, T., Zhao, P., Zhang, W., & Jiang, J. (2016). Ethanol production from a biomass mixture of furfural residues with green liquor-peroxide saccarified cassava liquid. BMC Biotechnol. 16(1), 1-11.

Kim, C., Jeong, D., Kim, S., Kim, Y., & Jung, S. (2019). Cyclodextrin functionalized agarose gel with low gelling temperature for controlled drug delivery systems. Carbohyd. Polym. 222, 115011.

Kim, J. H., Park, S., Kim, H., Kim, H. J., Yang, Y. H., Kim, Y. H., ... & Lee, S. H. (2017). Alginate/bacterial cellulose nanocomposite beads prepared using Gluconacetobacter xylinus and their application in lipase immobilization. Carbohyd. Polym. 157, 137-145.

Ullah, H., Wahid, F., Santos, H. A., & Khan, T. (2016). Advances in biomedical and pharmaceutical applications of functional bacterial cellulose-based

nanocomposites. Carbohyd. Polym. 150, 330-352.

Xu, L. M., Chen, L., Dong, Z., Wang, J., Wang, Z. J., & Shao, A. L. (2012). In vivo toxicity and in vitro cytotoxicity of silver nanoparticle based-hydrogel in reproductive organs of rabbit and Hela sells. Chin. J. Pharm. Anal. 32(2), 194-201.

Yan, H., Huang, D., Chen, X., Liu, H., Feng, Y., Zhao, Z., ... & Lin, Q. (2018). A novel and homogeneous scaffold material: preparation and evaluation of alginate/bacterial cellulose nanocrystals/collagen composite hydrogel for tissue engineering. Polym. Bull. 75(3), 985-1000.

Yuan, M., Bi, B., Huang, J., Zhuo, R., & Jiang, X. (2018). Thermosensitive and photocrosslinkable hydroxypropyl chitin-based hydrogels for biomedical applications. Carbohyd. Polym. 192, 10-18.